CONSTITUTIVE RELATIONS FOR PLASTIC DEFORMATION IN AA5754 SHEET

L. Hu[1], S. Banovic[2], T. Foecke[2] M. Iadicola[2], and A.D. Rollett[1]

[1] Department of Materials Science and Engineering
Carnegie Mellon University
5000 Forbes Avenue, Pittsburgh, PA 15213, USA
e-mail: LinHu@andrew.cmu.edu , rollett@andrew.cmu.edu

[2] NIST Center for Metal Forming
National Institute of Standards and Technology
Gaithersburg, MD 20899-8553, USA
e-mail: stephen.banovic@nist.gov , tfoecke@nist.gov, mark.iadicola@nist.gov

ABSTRACT

Constitutive equations for the multiaxial stress-strain behavior of aluminum alloy 5754 sheets have been developed, based on crystal plasticity. Both a Taylor-based polycrystal plasticity code (LApp) and a self-consistent viscoplastic code (VPSC) have been used to fit a single slip system hardening law to the available data for tension, plane strain and biaxial stretching. The fitting procedure yields good agreement with the monotonic stress-strain data. When the developed hardening law is used to model tests involving strain path changes, however, the agreement is less good. Furthermore, the simulated texture evolution is too rapid when compared to the experiments. These discrepancies motivate the further development of the constitutive relations to include such effects as grain-to-grain interactions and latent hardening.

Keywords: Forming; Simulation; Forming Limits; Constitutive Relations; Aluminum Alloys.

1. INTRODUCTION

5000-series Magnesium-strengthened Aluminum alloys are prospective materials for automotive interior surfaces. They have excellent weldability and corrosion resistance, providing a lower-weight alternative to steel with a boost in fuel economy, safety and driving performance [1]. Motivated by the need to manufacture parts efficiently from sheet aluminum metal, much research effort has been invested in studying basic mechanics involving metal forming.

Specifically, modeling on the plastic deformation in aluminum sheets can provide some insights into the forming process. The earliest work traces back to Hollomon's [2] empirical power law equation for uniaxial true stress–true plastic strain relationship of a material:

$$\sigma = K\varepsilon_p^n \qquad (1)$$

where σ is the stress, K is the strain hardening coefficient, ε_p is the plastic strain and n is the strain hardening exponent. Later studies on dislocation slip [3] help to identify various hardening stages in the plastic deformation of polycrystalline material, which brings the plasticity modeling to the grain scale. The constitutive relation involves the evolution of the hardening on individual slip system. The macroscopic behavior is then derived by taking average over all the grains. Such constitutive relations based on slip systems have been well established for monotonic loading. However, they are often inadequate to predict stress-strain curves and texture development for processes that involve different strain modes and multi-axial loading.

Two significant factors have drawn our attention in this study. The first factor is the intrinsic strain hardening due to dislocation accumulation. Various strain-hardening models have been proposed to describe hardening behaviors of a slip system such as isotropic hardening, latent hardening and kinematic hardening. However, it is still not clear whether the existing models are able to capture every important aspect of strain hardening, and to what extent we need to account for this complex dislocation interaction to be sufficiently accurate. The other factor is the interaction between grains, which has often been ignored in plasticity modeling. Non-uniform distributions of strain and stress across a deformed polycrystal [4] suggest the need for a more detailed description of grain interaction other than the common iso-strain [5] and iso-stress [6] assumptions.

In this study, simulations were undertaken using the Los Alamos Polycrystal Plasticity Packages (LApp) and Viscoplastic Self-consistent codes (VPSC). Mechanical tests are conducted on sheet alloy samples by collaborators at National Institute of Standards and Technology (NIST) to compare and validate the simulation work performed at CMU. The objective of the study is to establish equations that properly account for strain hardening and grain interaction behaviors during deformation. By incorporating such equations into current slip system based plasticity models, the accuracy of predictions for stress-strain curves and texture evolutions can be improved.

2. MATERIALS

5754 Aluminum Alloy is an Al-Mg alloy designed for structural and weldable sheets in vehicles such as inner body panels, splashguards, heat shields, air cleaner trays and covers, and load floors. Its chemical composition is reported in Table 1. The alloy derives its strength from the solid solution strengthening with magnesium atoms, interacting with dislocations and inhibiting dynamic recovery processes during straining. The addition of Manganese addition provides grain size control by forming well-dispersed particles. Also, for a given strength

requirement, the addition of manganese allows lower magnesium content and ensures a greater degree of stability of the alloy [7].

Table 1. *The chemical composition of AA5754 alloy used in this study.*

Element	Mg	Mn	Fe	Si	Cr, Cu, Pb, Ni, Sn, Ti, Zn	Aluminum
Weight Percent	3.75	0.29	0.24	0.06	Individually <0.05	Balance

The material used in this investigation was industrially processed AA5754-O sheet, nominally 1 mm thick. Figure 1 shows the microstructure of the RD/ND section of as-received material as observed by optical microscopy. The grains are relatively equiaxed in the rolling plane and slightly elongated along the RD. This is indicative of a recrystallized microstructure associated with the O-temper.
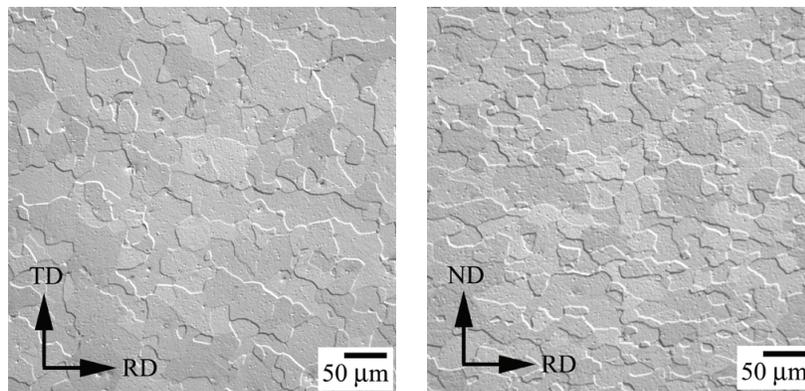

Figure 1. *Optical micrographs of as-received AA5754 sheet material showing a nearly equiaxed microstructure in both RD-TD and RD-ND cross-sections [8].*

3. EXPERIMENTAL PROCEDURE

3.1 Mechanical tests under single strain paths

Samples were cut to appropriate dimensions for testing and deformed in three strain states: uniaxial tension, plane strain and equibiaxial tension. Uniaxial deformation and plane strain testing were conducted with the sheet rolling direction parallel (RD-oriented) and perpendicular (TD-oriented) to the main stress axis. Thus, five mechanical tests were performed on the sample: RD-oriented and TD-oriented uniaxial tensile tests, RD-oriented and TD-oriented plane strain tests, and equibiaxial stretch test. Under all modes, samples were produced at approximately every 5 % true strain to near-failure.

The textures of the samples were measured using X-ray diffraction technique. Three incomplete pole figures were measured with $0° \leq \alpha \leq 65°$, namely: {111}, {200}, and {220}. The 3-D crystallite orientation distribution (COD) and full pole figures were derived from the pole figures using the preferred orientation package from Los Alamos (popLA). The COD was used to generate a weighted set of discrete orientations that are representative of the texture.

3.2 Mechanical tests with strain path changes

Mechanical tests with strain path changes were performed on the same material to study formability and which serve to investigate behaviors such as kinematic hardening and latent

hardening. The samples were first deformed in equibiaxial tension to a prescribed strain and then uniaxially tested parallel and perpendicular to the RD of the sheet respectively.

4. PLASTICITY SIMULATION

Two models were used to simulate the plastic response of the material. The initial texture is incorporated using a set of 1152 weighted orientations derived from the COD as previously described. The material parameters used in the actual simulations were identified by the best fit (root mean square error) of the experimental values and giving the same weight to all mechanical tests. This process is automated by using a UNIX shell script.

One of the simulations was done using LApp, a polycrystal plasticity code developed at Los Alamos National Laboratory. This model is used to calculate the stress state and texture evolution of applying a given strain rate to a set of orientations (grains). The basis of the simulation using LApp is the Taylor full constraint (FC) model where a uniform strain state is assumed. The strain hardening is modeled using the Voce law:

$$\theta = \theta_0 (1 - \tau/\tau_V) \qquad (2)$$

where θ_0 is the initial hardening rate and τ_v is the saturation critical resolved shear stress. In the analysis, the initial critical shear stress τ_0 and τ_v are respectively 65 MPa and 90 MPa.

The other simulation was performed using the viscoplastic self-consistent (VPSC) code developed by C. N. Tomé and R. A. Lebensohn at Los Alamos National Laboratory. Similar to the LApp model, this model is used to predict the stress-strain response and texture development in the polycrystalline material. The model treats each grain as a viscoplastic ellipsoidal inclusion embedded in a homogeneous elastic matrix (HEM). The properties of the matrix (HEM) are adjusted self-consistently to coincide with the average of all inclusions forming the aggregate. The tangent method [9] is adopted as the linearization scheme in the simulation. In contrast to the Taylor FC model, in the VPSC method, the strain in each grain can vary as a function of orientation, depending on the stiffness of the interaction. The extended Voce hardening law is used in the simulation:

$$\tau = \tau_0 + (\tau_1 + \theta_1 \Gamma)(1 - \exp(-\Gamma \theta_0 / \tau_1)) \qquad (3)$$

where τ_0, θ_0, θ_1, $(\tau_0 + \tau_1)$ are the initial CRSS, the initial hardening rate, the asymptotic hardening rate and the back-extrapolated CRSS. Parameters used in the simulation are: $\tau_0 = 33$ MPa, $\tau_1 = 98$ MPa, $\theta_0 = 285$ MPa, $\theta_1 = 0$. With $\theta_1 = 0$, the hardening equation reduces to the same form used in LApp.

5. RESULT AND DISCUSSION

5.1 Single-path mechanical test results

Figure 2 shows the stress-strain curves for AA5754 in the aforementioned five deformation modes simulated by LApp as well as those determined experimentally. In the uniaxial tension case, the stress in the direction of applied strain is measured. The predicted curves are in good agreement with experimental data from Figure 2a and 2b. Figure 2c and 2d shows respectively the stresses in the RD and TD directions versus strains for equibiaxial tension. LApp apparently overestimates experimental data with a faster work hardening. Figure 2e and 2f shows stress-strain curves for both longitudinal and transverse directions in plane strain tension where LApp tends to underestimate the flow stress in comparison to experiment.
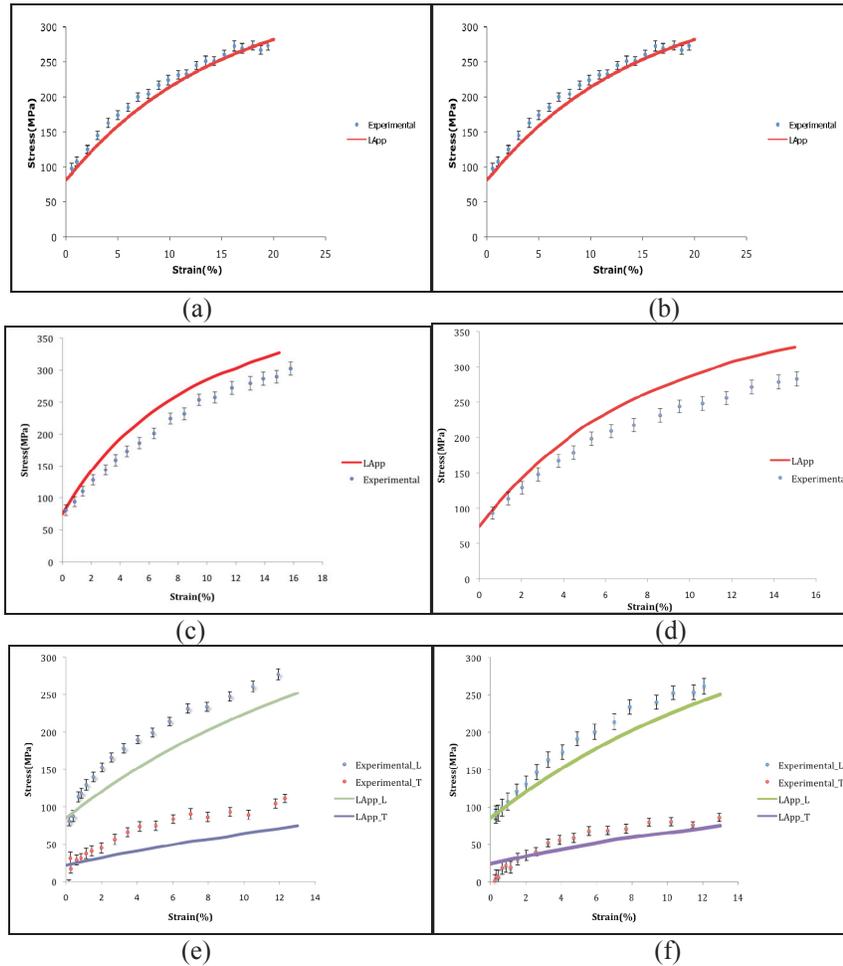
Figure 2. *Comparison of stress-strain curves measured in the experiments and predicted by Taylor FC model using the LApp code for different strain modes. (a) RD-oriented and (b) TD-oriented uniaxial tension; (c) along the RD and (d) TD direction for equibiaxial stretch; (e) RD-oriented and (f) TD-oriented plane strain.*

Figure 3 presents the fitting of simulated curves by VPSC with experimental stress-strain curves and it is apparent that the fitted curves match the data better than for the Taylor model. Since simulations so far have been done using a same hardening behavior in both LApp and VPSC, therefore, this shows that incorporating the grain interaction improves the modeling of plastic deformation. However, for the plane strain tension case, VPSC was only able to match one of the stresses accurately. The non-trivial deviation of calculated stresses from experimental data suggests the need to further analyze the strain hardening behavior and grain interaction effect.
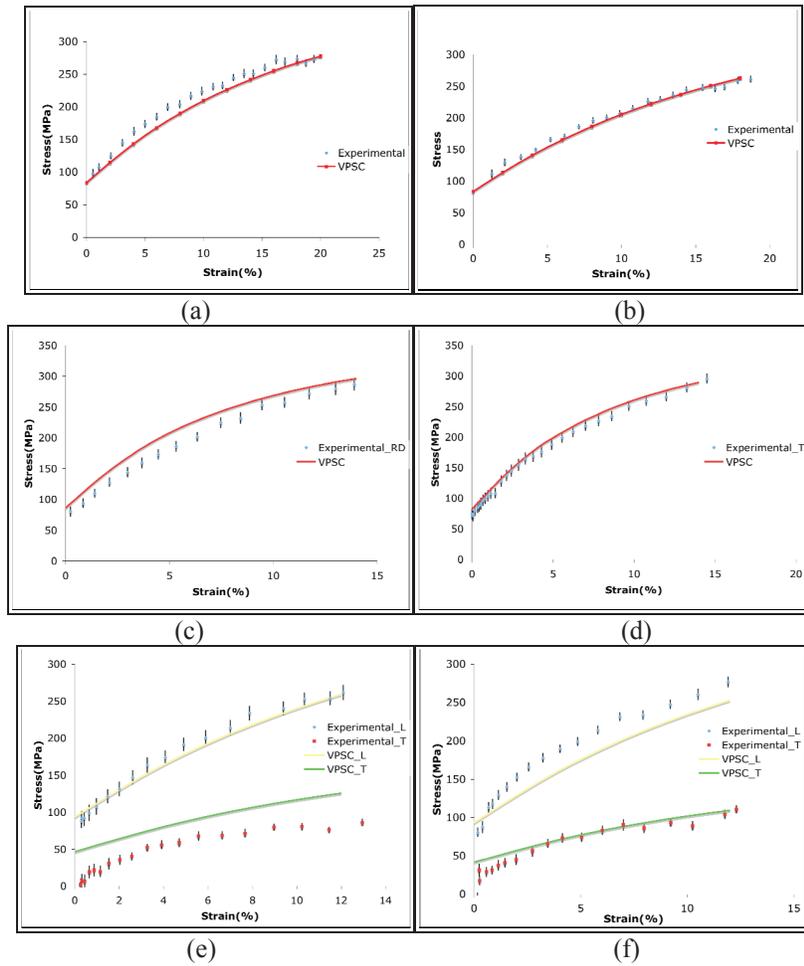
Figure 3. *Comparison of stress-strain curves measured in the experiments and predicted by VPSC for different strain modes. (a) RD-oriented uniaxial tension; (b) TD-oriented uniaxial tension; (c) along the RD and (d) TD direction for equibiaxial stretch; (f) TD-oriented plane strain.*

Figure 4 shows the recalculated {111} pole figures from the as-received materials for both RD- and TD-oriented samples. The sheet displays a low degree of texture with a combination of recrystallization (cube and S) and retained deformation (Brass and copper) components.
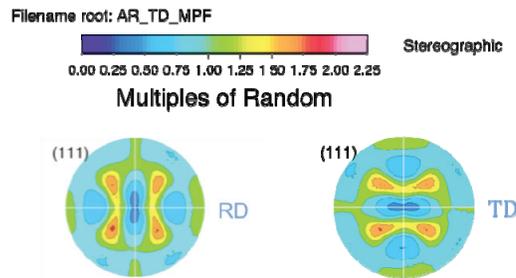

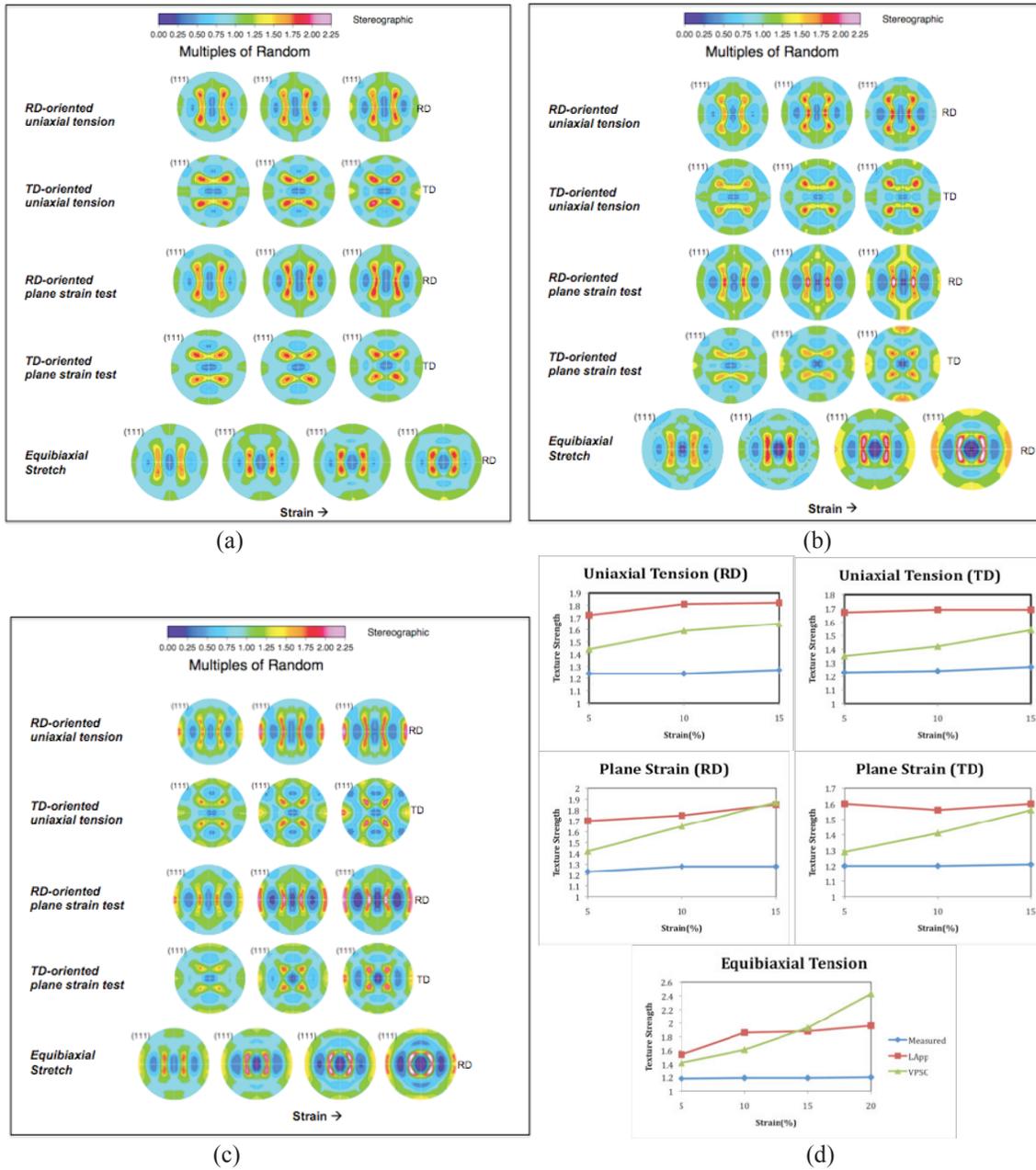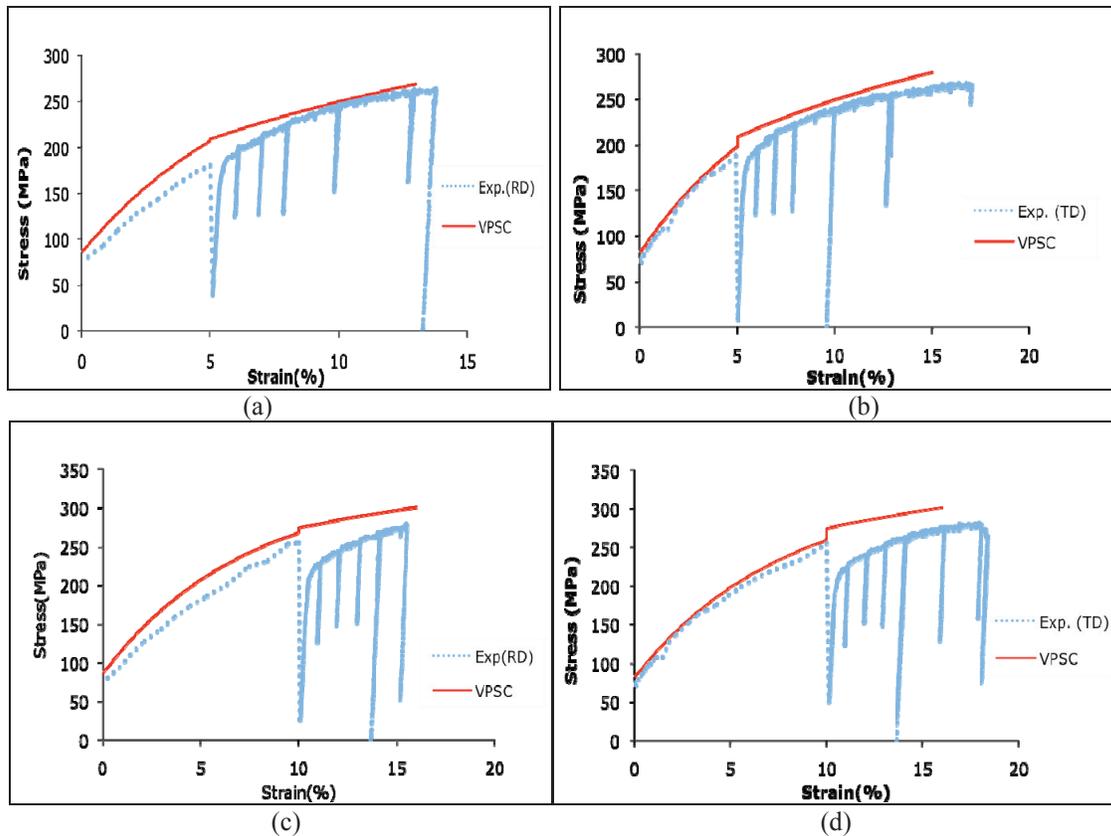**Figure 4.** *Recalculated {111} pole figures of as-received materials.*

Figure 5. *Evolution of {111} pole figures with strain level from (a) experiments and simulation by (b) LApp (c) and VPSC; in each figure, the strain levels 5%, 10% and 15% going from left to right, except for equibiaxial tension which also has 20%; (d) texture strength as a function of strain.*

Figure 5a shows the development of measured {111} pole figures as a function of deformation mode and strain level. Figure 5b and 5c are the corresponding pole figures simulated by LApp and by VPSC respectively. Pole figures from experiments and simulation are compared at the following equivalent von Mises strain levels: 5%, 10%, and 15% for uniaxial tension and plane strain; and 5%, 10%, 15% and 20% for equibiaxial tension. LApp and VPSC both predict correctly the sharpening of major as-received texture components. The plots of texture strength, Fig. 5d, show that VPSC predicts a weaker texture at low strains but a higher strengthening rate compared to LApp. In general, simulated textures strengthen significantly

with strain whereas the experimental textures barely change. This may be due to the neglect of the local neighborhood of individual grains in both models, which adds shears and rotations in order to maintain local compatibility and equilibrium.

5.2 Multipath mechanical test results

Figure 6 compares the experimental and theoretical stress-strain curves in the direction of applied uniaxial tension. For Figure 6(a), (c), (e) and (g), samples are loaded in RD-oriented uniaxial tension with a 5%, 10%, 15% and 20% biaxial prestrain, respectively. For Figure 6(b), (d), (f) and (h), samples are loaded in TD-oriented uniaxial tension with a 5%, 10%, 15% and 20% biaxial prestrain, respectively. The calculations were performed with the VPSC code using the same parameters fitted to the single path (monotonic straining) mechanical tests. In addition, isotropic hardening behavior and tangent type grain interaction are enforced. The VPSC code overestimates the flow stress for the beginning of uniaxial tension, especially as the prestrain increases. The softening phenomenon in the material when subjected to strain path changes may be associated with anisotropic hardening behaviors during the process. As currently implemented, the calculated stress-strain response shows a small increase in flow stress at the change in strain path, which is opposite to the observed decrease.
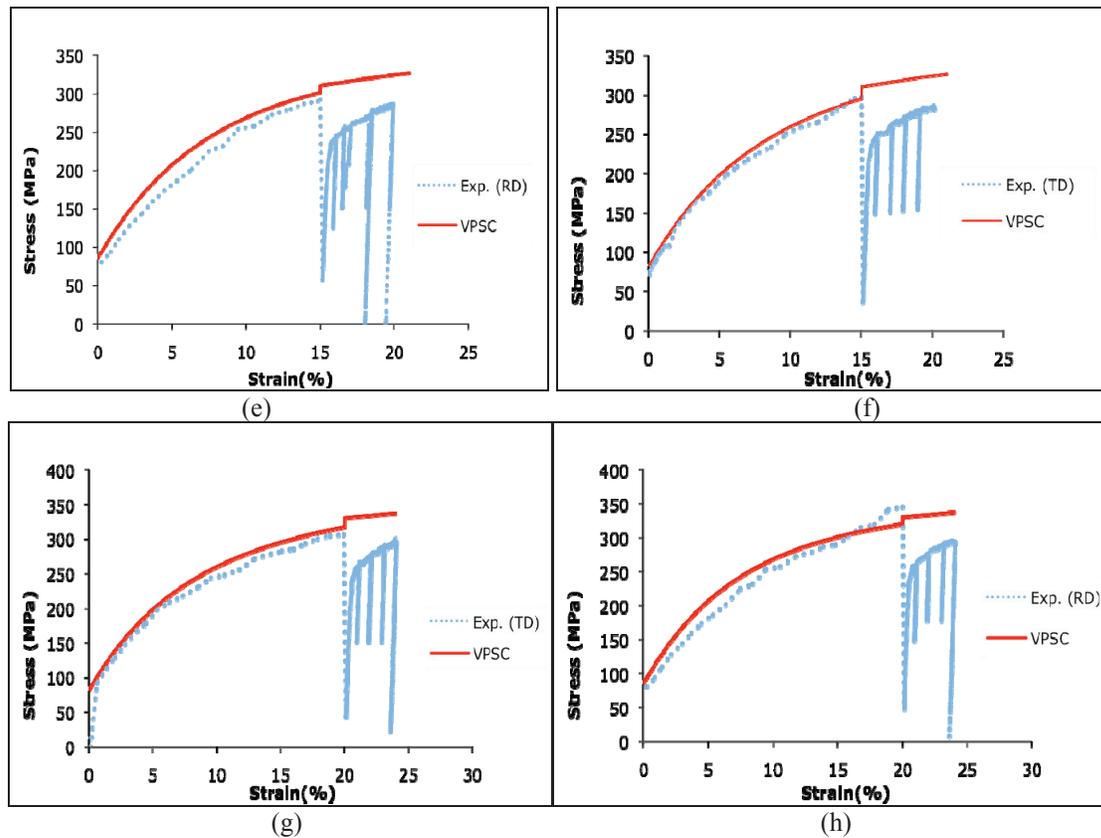

(a)

(b)

(c)

(d)

Figure 6. *Comparison of stress-strain curves measured from experiments and simulated by VPSC for RD-oriented tension after (a)5% (c) 10% (e) 15% (g) 20% biaxial prestrain; TD-oriented uniaxial tension after (b) 5% (d) 10% (f) 15% (h) 20% biaxial prestrain.*

6. CONCLUSIONS

Plastic deformation under various strain paths for AA5754 aluminum alloy has been calculated with both the LApp and VPSC codes. The single slip system hardening parameters have been fitted by comparison with the experimental stress-strain curves. Texture development has also been compared with experiments. The results indicate that taking grain interaction into consideration refines the polycrystal plasticity modeling. However, the failure to predict the mechanical response for multiaxial loading and strain path changes points out the need to find more effective ways to describe accurately the strain hardening and grain interaction.

7. ACKNOWLEDGEMENTS

8. REFERENCES

1. W. S. Miller, L. Zhuang, J. Bottema: "Recent development in aluminium alloys for the automotive industry", Materials Science and Engineering (2000) 37-49.
2. A. W. Bowen, P. G. Patridge: "Limitations of the Hollomon strain-hardening equation", J. Phys. D: Appl. Phys. 7 (1974) 969-978.
3. U. F. Kocks, H. Mecking: "Physics and phenomenology of strain hardening: the FCC case", Progress in Materials Science 48 (2003) 171–273.

4. S. Quilici and G. Cailletaud: "FE simulation of macro-, meso- and micro-scales in polycrystalline plasticity", Computational materials science 16 (1999) 383-390.
5. G. I. Taylor: "Plastic strain in metals", J. Inst. Metals (1938).
6. U. F. Kocks, C. Tomé, and H.-R. Wenk: Texture and Anisotropy, Cambridge University Press, Cambridge, 1998.
7. "ASM handbook Volume 2: Properties and Selection: Nonferrous Alloys and Special-Purpose Materials", ASM International (1990) 37-52.
8. S.W. Banovic, M.A. Iadicola, and T. Foecke: "Textural Development of AA 5754 Sheet Deformed under In-Plane Biaxial Tension", Metallurgical and Materials Transactions A (2008) 2246-2258.
9. C. N. Tomé: "Self-consistent polycrystal models: a directional compliance criterion to describe grain interactions", Modelling Simul. Mater. Sci. Eng. 7 (1999) 723-738.